IEEE Access
Multidisciplinary ⋮ Rapid Review ⋮ Open Access Journal

Received January 10, 2021, accepted January 18, 2021, date of publication January 29, 2021, date of current version February 8, 2021.

Digital Object Identifier 10.1109/ACCESS.2021.3055521

The Azimuthal Dependence of Exchange Bias Effect and Its Analysis by Spin Glass Model in $Ni_{0.8}Fe_{0.2}/Co_xNi_{1-x}O$ Bilayers

WOOSUK YOO[1], SEONGMIN CHOO[1], SINYONG JO[2], CHUN-YEOL YOU[3], JUNG-IL HONG[3], KYUJOON LEE[4], AND MYUNG-HWA JUNG[1]

[1]Department of Physics, Sogang University, Seoul 121-742, South Korea
[2]Department of Physics, Inha University, Incheon 402-752, South Korea
[3]Department of Emerging Materials Science, Daegu Gyeongbuk Institute of Science and Technology (DGIST), Deagu 711-873, South Korea
[4]Institute of Physics, Johannes Gutenberg University Mainz, 55099 Mainz, Germany

Corresponding authors: Kyujoon Lee (kyulee@uni-mainz.de) and Myung-Hwa Jung (mhjung@sogang.ac.kr)

This work was supported in part by the National Research Foundation of Korea (NRF) Grant funded by the Ministry of Education, Science and Technology (MEST), Korean Government under Grant 2016M3A7B4910400 and Grant 2020R1A2C3008044. The work of Kyujoon Lee was supported in part by the Graduate School of Excellence Materials Science in Mainz (MAINZ) GSC 266, MaHoJeRo, DAAD Spintronics network under Grant 57334897, in part by the German Research Foundation through SFB TRR 173 Spin + X project A01 under Grant 290319996/TRR173, and in part by the European Union's Horizon 2020 Research and Innovation Programme through the Marie Skłodowska-Curie Agreement under Grant 709151.

ABSTRACT Exchange bias (EB) effect has been vigorously researched for many years due to its possible applications in information storage and spintronics, especially in spin valves for magnetic recording devices. Even though many models have been expounded to this day, they do not prove convincingly the origins of EB effect. We attempt to establish the azimuthal dependence of EB effect with respect to varying the composition of the antiferromagnet $Co_xNi_{1-x}O$ and temperature. In this report, we deposited the bilayer thin films of $Ni_{0.8}Fe_{0.2}/Co_xNi_{1-x}O$ with x varying from 0.4 to 0.8 by magnetron sputtering and studied the variation of exchange bias field and coercivity. The EB effect was investigated for various external parameters such as temperature, the composition of antiferromagnetic layer, and the direction of magnetic field. The comparison between the calculations and experimental data showed good consistency with the spin glass model, and we suggest the validity of spin glass model to understand the origin of exchange bias effect in the $Ni_{0.8}Fe_{0.2}/Co_xNi_{1-x}O$ bilayers.

INDEX TERMS Spintronics, antiferromagnetic materials, anisotropic magnetoresistance.

I. INTRODUCTION

Since exchange bias (EB) effect was discovered by Meiklejohn and Bean in 1956 [1], [2], great interest has been shown to the phenomena due to it's possible applications in information storage and spintronics, especially in spin valves for magnetic recording devices. The EB effect is the induced unidirectional anisotropy mainly attributed to the interface between a ferromagnet (FM) and an antiferromagnet (AFM). When FM/AFM bilayer is cooled from the Néel temperature (T_N) of the AFM below the Curie temperature (T_C) of FM with an external magnetic field, a shift of hysteresis loop emerges in the opposite direction of field-cooling direction and the coercive field (H_C) increases compared to H_C before the field-cooling process. The magnitude of shift of hysteresis loop is called as EB field (H_{EB}). This EB effect has been widely used in magnetic devices especially pinning the fixed layer in read heads of hard disk drives. For these reasons understanding the underlying mechanism for EB effects is crucial.

The EB effect is caused by the interaction of interfacial spins between the FM and AFM. Although the EB effect has been studied for several decades, the origin of EB effect is still unsolved so that the essence of the EB effect remains unanswered because of the experimental difficulties by low interface to volume ratio of the FM and AFM interface. Although the phenomena of EB effect, for example, coercivity enhancement, training effect, temperature dependence, cooling field dependence, asymmetry of hysteresis loop, and vertical loop shift [3]–[8], are universally accepted, there is no

The associate editor coordinating the review of this manuscript and approving it for publication was Guijun Li.

general agreement about qualitative and quantitative analysis for EB effect. There have been many models stemming from the Stoner-Wolfram model in attempt to reveal the origin of EB effect. Among them only a few models, i.e. Meiklejohn and Bean model [1], Mauri model [9], [10], and spin glass model [10], [11], have been generally accepted in the research community. However still there are many controversies in selecting a model to explain the experimental results in different systems [12]–[16].

Various material systems are used as the AFM, such as IrMn [17]–[20], FeMn [21]–[23], CoO [24]–[27], and NiO [28], [29], for the EB. The most commonly used oxide AFMs for the EB systems are CoO and NiO. Here, CoO has a large anisotropy of 2.7×10^7 J/m^3 but the Néel temperature of $T_N = 291$ K which will not work at room temperatures. NiO has a high Néel temperature of $T_N = 563$ K but low anisotropy values of 6.16×10^5 J/m^3. Thus, in this study we use the alloyed system of CoO and NiO to tune the antiferromagnetic anisotropy (K_{AFM}) and the Néel temperature to achieve large exchange bias which work at room temperature. We have also tried to analyze the azimuthal dependence of H_{EB} and H_C with respect to the composition of CoO and NiO of the AFM [30]. Additionally, the temperature dependence from room temperature (300 K) to temperatures near the blocking temperature (T_B). Some studies reported that the EB effect has an azimuthal dependence of external magnetic field [11], [31]–[34], but so far there has been little studies on the azimuthal dependence with tuning of the AFM by changing the composition and measurement temperature. Especially, we measured H_{EB} and H_C by using the new approach by measuring the anisotropic magnetoresistance (AMR) [35]. We also discuss the qualitative agreement of EB measurements with the calculation based on the Mauri model and the spin glass model [10], [11]. The angular dependence of AMR was measured and fitted by the spin glass model and Mauri model. The results show that our measurements show qualitative agreement with the spin glass model. To verify this agreement with the spin glass, we additionally measured the temperature dependence of H_{EB} from extremely low temperature (5 K) to T_B and the training effect at 5 K.

II. EXPERIMENTAL DETAILS

$Co_xNi_{1-x}O$(60 nm)/$Ni_{0.8}Fe_{0.2}$(20 nm) (where $x = 0.3$, 0.4, 0.5, 0.6) bilayers were deposited *in-situ* at room temperature using magnetron sputtering method on the Si (100) substrate. The base pressure for the deposition was $< 5.0 \times 10^{-6}$ Torr. The AFM layer $Co_xNi_{1-x}O$ (60 nm) was deposited by RF magnetron sputtering in 2 mTorr of mixed argon and oxygen atmosphere using a Co_xNi_{1-x} target. The lattice parameter of $Co_xNi_{1-x}O$ is approximately 4.246 Å [36]. Subsequently, the FM layer $Ni_{0.8}Fe_{0.2}$ (20 nm) was deposited by DC magnetron sputtering in 2 mTorr of Argon using a $Ni_{0.8}Fe_{0.2}$ target. All the samples were capped with 5 nm of SiO_2. The thickness and roughness of each layers were confirmed by measuring X-ray reflectivity (XRR) measurements as shown in Fig. 1a. The samples are textured and crystalized, which is determined from the XRR data as shown in Fig. 1a. We measured magnetic field vs magnetization curve using a vibrating sample magnetometer-superconducting quantum interference device (VSM-SQUID) at 300 K. All samples have an in-plane magnetic anisotropy so that all the measurements were done with the magnetic field applied in the in-plane direction of the film. We analyzed azimuthal angular dependence of H_{EB} and H_C by measuring the AMR [35]. The AMR was measured by using the Wan der Pauw method as shown in Fig. 1c. We used indium to make contacts for AMR measurements. All the samples were heated to temperature 473 K which is greater than T_N (= 417 K in $Co_{0.52}Ni_{0.48}O$) of $Co_xNi_{1-x}O$ [35], [36] and lower than T_C (= 850 K) of $Ni_{0.8}Fe_{0.2}$ [37], and then cooled to room temperature (approximately 300 K) in external field of 200 Oe parallel to the applied current direction for the field cooling. After the field-cooling process, AMR of the samples was measured by using a measurement system equipped with three-dimensional magnets at 300 K, 333 K, and 353 K temperatures lower than T_B (approximately 370 K) [10] with rotating the external magnetic field from 0 to 360°. The external magnetic field was swept from −200 Oe to +200 Oe in the indicated direction. The measurement system can be operated only above room temperature therefore we have done the measurements above 300 K. We extracted the exchange bias field (H_{EB}) and coercive field (H_C) by using a method analyzing the AMR as described in Ref. 35. In Fig. 1d, we have plotted an AMR sweep of $x = 0.5$ measured in the direction of 45° in comparison to the hysteresis loop measured by the magnetization measurements. We measured the H_{C1} and H_{C2} by finding the crossing points of the AMR data with the extended line (marked with dotted lines) of the AMR value when the magnetization is saturated as shown in Fig. 1d. From these AMR measurements we could extract H_C and H_{EB}. The azimuthal angle was defined relative to the direction of the cooling field. We also observed temperature dependence from 360 to 5 K after field-cooling process and the training effect at 5 K by using a measurement system equipped with one-dimensional magnet which can be operated from 5 to 360 K. The temperature dependence was measured for the field cool direction $\theta = 0°$. The training effect was measured at 5 K due to the negligible training effect above room temperature.

III. RESULTS AND DISCUSSION

We measure H_{EB} and H_C for all the samples of $Co_xNi_{1-x}O/Ni_{0.8}Fe_{0.2}$ for various compositions ($x = 0.3$, 0.4, 0.5, and 0.6) while rotating the applied magnetic field direction from $\theta = 0$ to 360°, where θ is the angle between the applied magnetic field and field-cooling (FC) direction as shown in Fig. 1b. Fig. 1d shows a representative hysteresis loop of the field cooled sample of $x = 0.5$ at 300 K showing that $Ni_{0.8}Fe_{0.2}$ layer is a soft ferromagnet. There is a clear shift

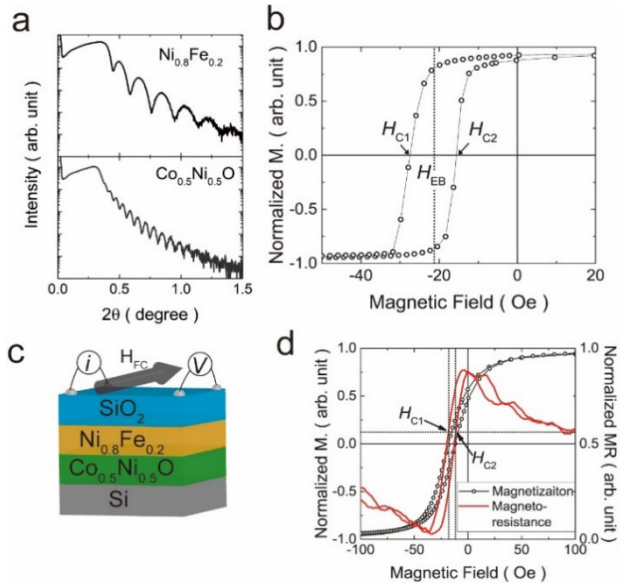

FIGURE 1. (a) X-ray reflectivity patterns of each $Ni_{0.8}Fe_{0.2}$ and $Co_{0.5}Ni_{0.5}O$ layer. (b) Magnetization curve of $x = 0.5$ sample and definition of H_{C1}, H_{C2} and H_{EB}. (c) Schematic drawing of the bilayer with the configuration of the measurement. The black arrow represents the direction of the applied magnetic field during field cooling. The i is the applied current and V is the measured voltage for the magnetoresistance measurements. (d) Representative hysteresis loop of $x = 0.5$ at $T = 300$ K measured after field cooling the sample.

of the hysteresis loop to the left of the $H = 0$. This means that by the FC we have induced the EB effect in our system. Here, we define the H_{EB} and H_C by $H_{EB} = (H_{C1} + H_{C2})/2$ and $H_C = (H_{C2} - H_{C1})/2$, respectively, where H_{C1} and H_{C2} are the two switching fields as shown in Fig. 1b. The training effect and temperature dependence of H_{EB} have been measured for $Co_{0.5}Ni_{0.5}O/Ni_{0.8}Fe_{0.2}$ films.

Fig. 2a show the azimuthal dependence of H_{EB} for the samples of different compositions measured at room temperature. The overall angular dependence behaviors show a sinusoidal form. Here it is noticeable that the amplitude of the H_{EB} is different for different x which is due to the different Néel temperature and AFM properties of individual compositions. The overall behavior of the angular dependence of H_{EB} for $x = 0.3$ and 0.6 exhibit a plateau like behavior which is due to the change in the parameters of the AFM leading to a deformation in the H_{EB} angular dependence. In order to better understand the EB of these materials we have performed calculations for the azimuthal dependence of H_{EB} by two different models, the Mauri model and the spin glass model, because the modified Stoner-Wolfram model and the generalized Meiklejohn and Bean model are simple forms of the spin glass model which neglect the term associated to the disorder of the interfacial spins. The Mauri model considers domain wall developed in the AFM to reduce H_{EB} computed from the Meiklejohn and Bean model [9], [10]. The total magnetic energy for the Mauri model can be described as [10]:

$$E = -\mu_0 H M_{FM} t_{FM} \cos(\theta - \beta) + K_{FM} t_{FM} \sin^2(\beta) - J_{EB} \cos(\beta - \alpha) - 2\sqrt{A_{AFM} K_{AFM}}(1 - \cos(\alpha)) \quad (1)$$

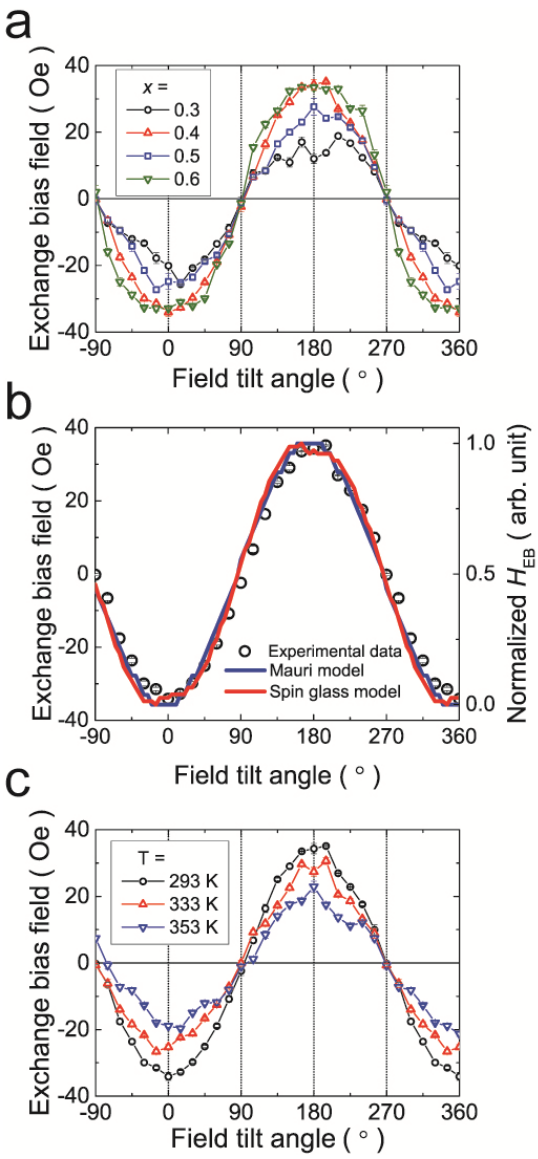

FIGURE 2. (a) Azimuthal dependence of H_C for different composition x, where the angle θ is the angle of the applied magnetic field during the measurement relative to the field-cooling external field direction. (b) experimental and calculation results of the azimuthal dependence of H_C for $x = 0.4$. The solid lines are the calculation results based on the Mauri model and the spin glass model. (c) Temperature dependence for the azimuthal dependence of H_C for $x = 0.4$.

where H is the external magnetic field, M_{FM} is the saturation magnetization of FM, t_{FM} is the thickness of FM, and K_{FM} is the anisotropy of FM. A_{AFM} is the exchange stiffness, α is the angle between the anisotropy of AFM and the interfacial AFM spins, and β is the angle between the anisotropy of FM and the FM spins in the external magnetic field H as illustrated in Fig. 5a. The first term is the Zeeman energy of the FM layer, the second term is the anisotropy energy of the FM layer, the third term is the interfacial exchange interaction, and the fourth term is the energy of domain wall at the interface between FM and AFM layers.

The spin glass model [10], [11] assumes that the spin glass like system at the interface between FM and AFM.

This model supposes the AFM layer has two types of AFM spins: one is frozen and uncompensated spins with large anisotropy and the other is rotatable spins with low anisotropy. In the spin glass model, the total magnetic energy can be written as [10]:

$$\begin{aligned} \mathrm{E} = & -\mu_0 H M_{FM} t_{FM} \cos(\theta - \beta) + K_{FM} t_{FM} \sin^2(\beta) \\ & - K_{AFM} t_{AFM} \sin^2(\alpha) + K_{SG}^{eff} \sin^2(\beta - \gamma) \\ & - J_{EB}^{eff} \cos(\beta - \gamma) \end{aligned} \tag{2}$$

where $K_{\mathrm{SG}}^{\mathrm{eff}}$ is the effective uniaxial spin glass anisotropy, $J_{\mathrm{EB}}^{\mathrm{eff}}$ is the reduced interfacial exchange energy, and γ is the average angle of the effective spin glass anisotropy as illustrated in Fig. 5b. $K_{\mathrm{SG}}^{\mathrm{eff}} = (1-f)J_{\mathrm{EB}}$ and $J_{\mathrm{EB}}^{\mathrm{eff}} = fJ_{\mathrm{EB}}$, where f means the degree of disorder at the interface such that $f = 1$ implies a perfect interface and $f = 0$ indicates 100% disorder. The first term is the Zeeman energy of the FM layer, the second term is the anisotropy energy of the FM layer, the third term is the anisotropy energy of the AFM layer, the fourth term is the effective anisotropy energy of the frustrated spins in the interfacial AFM layer, and the fifth term is the interfacial exchange interaction energy of the frustrated spins.

Using (1) and (2), we calculated the hysteresis loops for different azimuthal angles and extracted the H_{EB} and H_{C} values by varying the parameters such as K_{AFM} and found calculation results with qualitative agreement to the experimental results. We used $M_{\mathrm{FM}} = 8.6 \times 10^5$ A/m and $K_{\mathrm{FM}} = 5.0 \times 10^{-3}$ J/m^3 which are the values for permalloy $Ni_{0.8}Fe_{0.2}$, and $t_{\mathrm{FM}} = 20$ nm and $t_{\mathrm{AFM}} = 60$ nm which is the thickness of FM and AFM layer, relatively. The parameter K_{AFM} varies on the composition x, so we used an estimated range of 1.0×10^7 J/m^3 to 7.0×10^7 J/m^3 from the K_{AFM} of CoO which is 2.7×10^7 J/m^3 from Ref. 10. $A_{\mathrm{AFM}} = 6.97 \times 10^{-13}$ J/m, which is the A_{AFM} value for CoO [10], [38], was used in the calculations since we assume that the exchange stiffness does not vary drastically in our samples. Fig. 2b displays the comparison of our experimental data with the calculated H_{EB} data for the azimuthal dependent behaviors in $x = 0.4$. We have theoretically studied all the samples and representatively show the data for x = 0.4 which shows the largest angular dependence of the exchange bias field. The fitting parameters for all the compositions are displayed in Table 1. The data from both models show qualitative agreement with the measured data. In Table 1 we have presented the parameters from the calculation which match best with the experimental data. In the later sections we will discuss the details of the parameters along with the reason we have not presented the parameters for the Mauri model. In Fig. 2c, the temperature dependence of the azimuthal dependent H_{EB} is plotted for $x = 0.4$. We have measured at selected temperatures, $T = 293$ K, 333 K, and 353 K, up to the blocking temperature. There are no significant changes in the shape of the azimuthal dependence but only a decrease in the overall amplitude as the temperature increases which is due to the decrease of the EB strength when the temperature reaches the blocking temperature.

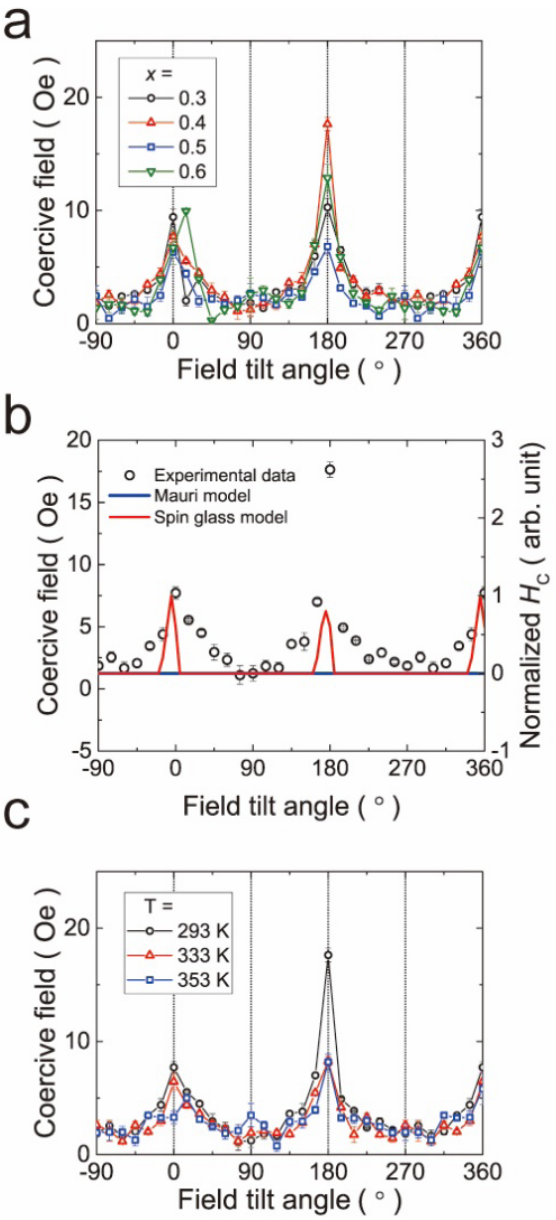

FIGURE 3. (a) Azimuthal dependence of the exchange bias field H_{EB} for different composition x, where the angle θ is the angle of the applied magnetic field during the measurement relative to the field cool magnetic field direction. (b) Experimental and calculation results of the azimuthal dependence of H_{EB} for $x = 0.4$. The solid lines are the calculation results based on the Mauri model and the spin glass model. (c) Temperature dependence for the Azimuthal dependence of H_{EB} for $x = 0.4$.

The measured azimuthal-dependent H_{C} for different compositions at room temperature is shown in Fig. 3a. The overall behavior does not change for the different x. All graphs of different x exhibit a peak value at angles $\theta = 0$, 180, and 360°. Thus, the different compositions do not change the qualitative behavior of the H_{C} by the EB effect. Additionally, we compare the calculated azimuthal angle dependent H_{C} values with the measured data. In Fig. 3b the experimental data of $x = 0.4$ is plotted with the normalized H_{C} values

from the calculations. Here, the Mauri model cannot reproduce the angular dependent behavior of H_C with a peak at angles $\theta = 0$, 180, and 360°. However, the spin glass model explicitly explains the azimuthal dependence and temperature dependence of H_C as introducing frozen and rotatable spins [10], [11]. Thus, in our system the spin glass model coincides with the behavior of the azimuthal dependence of H_C. The temperature dependence of the angular dependent H_C in $x = 0.4$ is plotted in Fig. 3c. The overall behavior does not change over a change in the temperature. Even the amplitude of H_C exhibits little change implying the possibility that the magnetic property of the permalloy has negligible temperature dependence.

In order to find further evidence of the spin glass model, we have measured the temperature dependence of the coercive field (H_C) and the exchange bias field (H_{EB}) as shown in Fig. 4a. For the full temperature dependence, we could not measure the full angular dependence due to the limitations of our system. We have measured the temperature dependence for the field sweep in the direction of $\theta = 0$. The temperature dependence of H_C shows an increase with decreasing temperature from 360 to 5 K which is a general behavior of the coercive field in exchange bias systems. The temperature dependence of H_{EB} shows two steps of drastic increase in low temperature below 50 K and high temperature range above room temperature. There is a plateau in a wide range of temperature from 50 to 270 K. This temperature dependence is similar to that of NiO-$NiFe_2O_4$ system [39]. This tendency of a plateau in the temperature dependence can appear when the domain wall energy at the interface is greater than the interfacial coupling energy described by the Stiles-McMichael model [40]. This model assumes random orientation of antiferromagnetic grains which can act like disordered spins at the interface in the spin glass model. Therefore, we speculate the existence of rotatable spins with low anisotropy by the antiferromagnetic grains at the interface.

In Fig. 4b, we plot the exchange bias field versus the number of repeated loops that were measured after the field cooling to measure the training effect at 5 K. We have fitted the data by equation (3) considering the single spin reversal (SSR) mode and the collective spin cluster rotation (CSR) mode [39], [41]. The training effect can be fitted by a hybrid function consisted of an exponential function for a fast decaying (CSR mode) and a $n^{1/2}$ function that is suitable for the gradual decaying (SSR mode) which sums up to be [41],

$$H_E(n) = H_0 e^{-(n-1)/\tau} + H_1 n^{-1/2} + H_E^{\infty} \qquad (3)$$

where H_0 and H_1 represent the CSR and SSR components of the training effect, respectively. H_E^{∞} is the exchange bias field after infinite cycles, and τ is a relaxation time. The fast decay is attributed to the rearrangement of frustrated AFM spins, in other words, the rotatable spins in the spin glass model and the gradual decay is caused by the frozen interfacial spins [39], [41] which implies that the exchange

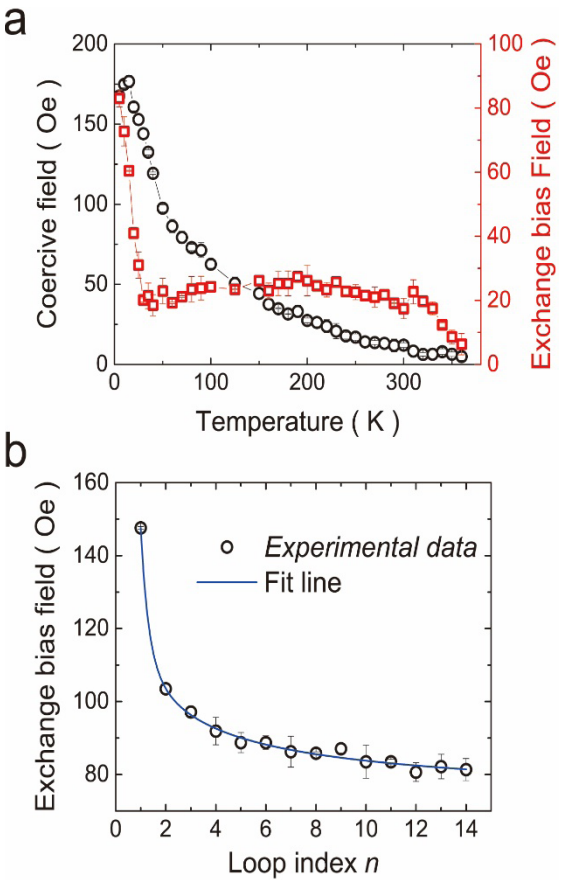

FIGURE 4. (a) Temperature dependence of the coercive fields and the exchange bias field which is measured after sufficient repetitions of the loop to remove the training effect. (b) Training effect of exchange bias fields measured by measuring the hysteresis loops repeatedly at 5 K.

bias in our system has contributions from spin glass states at the interface.

To verify whether the Mauri model or the spin glass model is valid for describing EB by using another method, the azimuthal dependence of the AMR can be used. Firstly, we measured the AMR of $x = 0.5$ at 300 K with a fixed external magnetic field of 100 Oe and vary the azimuthal angle. The data is fitted by both the Mauri model and the spin glass model. In Fig. 5c we plot the measured data and the fitting results by the Mauri model and the spin glass model. The experimental data show a behavior similar to $\cos^2\theta$ function which is the normal AMR behavior in polycrystalline FMs [42]. However, the experimental data does not exactly coincide with $\cos^2\theta$. This can be attributed to the change in the magnetization angle of FM spins at the interface caused by EB. Therefore, we fitted our experimental data by reflecting the tilt in the magnetization angle by using the total magnetic energy of both the Mauri model and the spin glass model as described in (1) and (2).

In Fig. 5c, our experimental AMR data was fitted by varying f from 0 to 1 and γ from 0° to 360°. The fitted curve by the Mauri model do not coincide with the measured data. On the other hand, the best fitted curve is found with $K_{AFM} = 5.0 \times 10^7$ J/m^3, $\gamma = 20°$ and $f = 0.8$ by

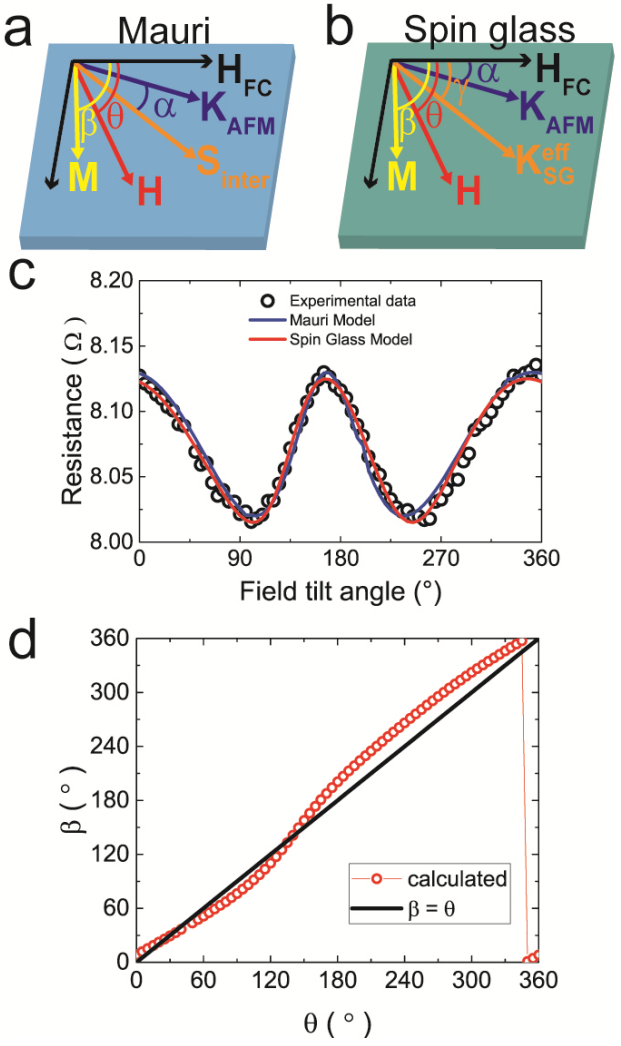

FIGURE 5. (a) Definition of angles and vectors assumed in Mauri models and (b) in spin glass model. (c) Anisotropic magnetoresistance measured while applying an external field of 100 Oe. The solid lines are the fitting lines by the Mauri model (blue line) and the spin glass model (red line). (d) Azimuthal angular dependence of the calculated magnetization tilt angle β. The solid black line represents the case when $\beta = \theta$.

the spin glass model. Therefore, the Mauri model cannot appropriately explain EB in our system, and the spin glass model best describes the AMR changed by EB, and this provides another evidence that possibly the spin glass model can shed light on the origin of EB. Fig. 5d shows the relation between θ and β where the solid line describes the case when the AMR shows a cosine squared behavior. The magnetization M_{FM} direction is different from the direction of the applied external magnetic field H, because the direction of the effective spin glass anisotropy does not exactly match with the anisotropy in the FM.

In table 1, we have summarized the parameters γ and f obtained from the azimuthal dependence of H_{EB} and the AMR fitting of all the samples measured at 300 K by the spin glass model. Overall, the γ and f values obtained from the two different measurements agree. The f values are in the range of 0.7-0.9 meaning small portions of disorder has to be

TABLE 1. The parameters γ and f obtained from the simulation of azimuthal dependence of H_{EB} and the AMR fitting of all the samples measured at 300 K by the spin glass model in all the samples $x = 0.3$, 0.4, 0.5, and 0.6.

	from H_{EB} and H_C calculation		from AMR fitting	
x	γ (°)	f	γ (°)	f
0.3	180	0.7	175	0.7
0.4	5	0.9	5	0.9
0.5	20	0.9	20	0.8
0.6	0	0.8	0	0.7

taken into account. Although there are differences in some of the values for the different methods the discrepancy is small. This might be due the fact that the changes in the γ and f does not drastically change the fitting or calculated results especially in the realistic range of f values. Therefore, more studies are required to conclude that the spin glass model can explain the EB in our system, but we provide some evidence from the two different measurements that the spin glass model can better explain our results.

IV. CONCLUSION

In this manuscript we have attempted to analyze the azimuthal and temperature dependence of H_{EB} and H_C in various compositions, x, of $Co_xNi_{1-x}O$. The H_{EB} and H_C were calculated based on two different models, the Mauri model, and the spin glass model, to explain the measured results. Both Mauri model and spin glass model well describe the azimuthal dependence of H_{EB}, but only the spin glass model can explain the azimuthal dependence in H_C. These results well agree with the fitting of the AMR measurements where the fitting has discrepancies according to the Mauri model but well agrees with the spin glass model. Especially, the calculated parameters γ and f well agree for the two different methods. Thus, we conclude that the spin glass model can better explain the results of our measurements and can be a more realistic model for our material system.

REFERENCES

[1] W. H. Meiklejohn and C. P. Bean, "New magnetic anisotropy," *Phys. Rev.*, vol. 102, no. 5, pp. 1413–1414, Jun. 1956.
[2] W. H. Meiklejohn and C. P. Bean, "New magnetic anisotropy," *Phys. Rev.*, vol. 105, no. 3, pp. 904–913, Feb. 1957.
[3] J. Nogués and I. K. Schuller, "Exchange bias," *J. Magn. Magn. Mater.*, vol. 192, pp. 203–232, Feb. 1999.
[4] R. L. Stamps, "Mechanisms for exchange bias," *J. Phys. D, Appl. Phys.*, vol. 34, no. 3, p. 444, Feb. 2001.
[5] M. Kiwi, "Exchange bias theory," *J. Magn. Magn. Mater.*, vol. 234, no. 3, pp. 584–595, Sep. 2001.
[6] K. O'Grady, L. E. Fernandez-Outon, and G. Vallejo-Fernandez, "A new paradigm for exchange bias in polycrystalline thin films," *J. Magn. Magn. Mater.*, vol. 322, no. 8, pp. 883–899, Apr. 2010.
[7] S. Giri, M. Patra, and S. Majumdar, "Exchange bias effect in alloys and compounds," *J. Phys. Condens. Matter*, vol. 23, no. 7, Feb. 2011, Art. no. 073201.
[8] Ò. Iglesias, A. Labarta, and X. Batlle, "Exchange bias phenomenology and models of core/shell nanoparticles," *J. Nanoscience Nanotechnol.*, vol. 8, no. 6, pp. 2761–2780, Jun. 2008.

[9] D. Mauri, H. C. Siegmann, P. S. Bagus, and E. Kay, "Simple model for thin ferromagnetic films exchange coupled to an antiferromagnetic substrate," *J. Appl. Phys.*, vol. 62, no. 7, pp. 3047–3049, Oct. 1987.

[10] F. Radu and H. Zabel, "Exchange bias effect of ferro-/antiferromagnetic heterostructures," in *Magnetic Heterostructures*, vol. 3, 1st ed. Berlin, Germany: Springer, 2008, pp. 97–184.

[11] F. Radu, A. Westphalen, K. Theis-Bröhl, and H. Zabel, "Quantitative description of the azimuthal dependence of the exchange bias effect," *J. Phys., Condens. Matter*, vol. 18, no. 3, pp. L29–L36, Jan. 2006.

[12] B. H. Miller and E. D. Dahlberg, "Use of the anisotropic magnetoresistance to measure exchange anisotropy in Co/CoO bilayers," *Appl. Phys. Lett.*, vol. 69, no. 25, pp. 3932–3934, Dec. 1996.

[13] S. G. E. te Velthuis, A. Berger, G. P. Felcher, B. K. Hill, and E. D. Dahlberg, "Training effects and the microscopic magnetic structure of exchange biased Co/CoO bilayers," *J. Appl. Phys.*, vol. 87, no. 9, pp. 5046–5048, May 2000.

[14] F. Radu, M. Etzkorn, V. Leiner, T. Schmitte, A. Schreyer, K. Westerholt, and H. Zabel, "Polarised neutron reflectometry study of Co/CoO exchange-biased multilayers," *Appl. Phys. A, Mater. Sci. Process.*, vol. 74, pp. 1570–1572, Dec. 2002.

[15] U. Welp, S. G. E. te Velthuis, G. P. Felcher, T. Gredig, and E. D. Dahlberg, "Domain formation in exchange biased Co/CoO bilayers," *J. Appl. Phys.*, vol. 93, no. 10, pp. 7726–7728, May 2003.

[16] F. Radu, M. Etzkorn, R. Siebrecht, T. Schmitte, K. Westerholt, and H. Zabel, "Interfacial domain formation during magnetization reversal in exchange-biased CoO/Co bilayers," *Phys. Rev. B, Condens. Matter*, vol. 67, no. 13, Apr. 2003, Art. no. 134409.

[17] A. Kohn, A. Kovács, R. Fan, G. J. McIntyre, R. C. C. Ward, and J. P. Goff, "The antiferromagnetic structures of $IrMn_3$ and their influence on exchange-bias," *Sci. Rep.*, vol. 3, no. 1, p. 2412, Dec. 2013.

[18] J. Feng, H. F. Liu, H. X. Wei, X.-G. Zhang, Y. Ren, X. Li, Y. Wang, J. P. Wang, and X. F. Han, "Giant perpendicular exchange bias in a subnanometer inverted (Co/Pt)n/Co/IrMn structure," *Phys. Rev. A, Gen. Phys.*, vol. 7, no. 5, May 2017, Art. no. 054005.

[19] C. Y. Tsai, J.-H. Hsu, and K. F. Lin, "Perpendicular exchange bias behaviors of CoPt/IrMn and CoPt/FeMn bilayers: A comparative study," *J. Appl. Phys.*, vol. 117, no. 17, May 2015, Art. no. 17D153.

[20] J. Sort, V. Baltz, F. Garcia, B. Rodmacq, and B. Dieny, "Tailoring perpendicular exchange bias in [Pt/Co]-IrMn multilayers," *Phys. Rev. B, Condens. Matter*, vol. 71, no. 5, Feb. 2005, Art. no. 054411.

[21] X. P. Zhao, J. Lu, S. W. Mao, Z. F. Yu, D. H. Wei, and J. H. Zhao, "Spontaneous perpendicular exchange bias effect in L10-MnGa/FeMn bilayers grown by molecular-beam epitaxy," *Appl. Phys. Lett.*, vol. 112, no. 4, Jan. 2018, Art. no. 042403.

[22] N. N. Phuoc and T. Suzuki, "Perpendicular exchange bias mechanism in FePt/FeMn multilayers," *J. Appl. Phys.*, vol. 101, no. 9, May 2007, Art. no. 09E501.

[23] H.-C. Choi, C.-Y. You, K.-Y. Kim, J.-S. Lee, J.-H. Shim, and D.-H. Kim, "Antiferromagnetic layer thickness dependence of noncollinear uniaxial and unidirectional anisotropies in NiFe/FeMn/CoFe trilayers," *Phys. Rev. B, Condens. Matter*, vol. 81, no. 22, Jun. 2010, Art. no. 224410.

[24] P. Kappenberger, S. Martin, Y. Pellmont, H. J. Hug, J. B. Kortright, O. Hellwig, and E. E. Fullerton, "Direct imaging and determination of the uncompensated spin density in exchange-biased CoO/(CoPt) multilayers," *Phys. Rev. Lett.*, vol. 91, no. 26, Dec. 2003, Art. no. 267202.

[25] Y. Ijiri, T. C. Schulthess, J. A. Borchers, P. J. van der Zaag, and R. W. Erwin, "Link between perpendicular coupling and exchange biasing in Fe_3O_4/CoO multilayers," *Phys. Rev. Lett.*, vol. 99, no. 14, Oct. 2007, Art. no. 147201.

[26] A. N. Dobrynin and D. Givord, "Exchange bias in a Co/CoO/Co trilayer with two different ferromagnetic-antiferromagnetic interfaces," *Phys. Rev. B, Condens. Matter*, vol. 85, no. 1, Jan. 2012, Art. no. 014413.

[27] K. Takano, R. H. Kodama, A. E. Berkowitz, W. Cao, and G. Thomas, "Interfacial uncompensated antiferromagnetic spins: Role in unidirectional anisotropy in polycrystalline $Ni_{81}Fe_{19}$/CoO bilayers," *Phys. Rev. Lett.*, vol. 79, no. 6, pp. 1130–1133, Aug. 1997.

[28] T. Gao, N. Itokawa, J. Wang, Y. Yu, T. Harumoto, Y. Nakamura, and J. Shi, "Off-easy-plane antiferromagnetic spin canting in coupled FePt/NiO bilayer structure with perpendicular exchange bias," *Phys. Rev. B, Condens. Matter*, vol. 94, no. 5, Aug. 2016, Art. no. 054412.

[29] Y. Wang, J. Xiong, Y. Zhang, L. Sun, B. You, J. Du, A. Hu, and M. Lu, "The effects of co-metal clusters on exchange bias for co-doped NiO/FeNi bilayers," *Appl. Surf. Sci.*, vol. 252, no. 24, pp. 8611–8614, Oct. 2006.

[30] M. J. Carey and A. E. Berkowitz, "Exchange anisotropy in coupled films of $Ni_{81}Fe_{19}$ with NiO and $Co_xNi_{1-x}O$," *Appl. Phys. Lett.*, vol. 60, no. 24, pp. 3060–3062, Jun. 1992.

[31] T. Ambrose, R. L. Sommer, and C. L. Chien, "Angular dependence of exchange coupling in ferromagnet/antiferromagnet bilayers," *Phys. Rev. B, Condens. Matter*, vol. 56, no. 1, pp. 83–86, Jul. 1997.

[32] H. Xi and R. M. White, "Angular dependence of exchange anisotropy in $Ni_{81}Fe_{19}$/CrMnPtx bilayers," *J. Appl. Phys.*, vol. 86, no. 9, pp. 5169–5174, Nov. 1999.

[33] J.-G. Hu, G.-J. Jin, and Y.-Q. Ma, "Thickness and angular dependencies of exchange bias in ferromagnetic/antiferromagnetic bilayers," *J. Appl. Phys.*, vol. 92, no. 2, pp. 1009–1013, Jul. 2002.

[34] H.-C. Choi, C.-Y. You, K.-Y. Kim, J.-S. Lee, J.-H. Shim, and D.-H. Kim, "Antiferromagnetic layer thickness dependence of noncollinear uniaxial and unidirectional anisotropies in NiFe/FeMn/CoFe trilayers," *Phys. Rev. B, Condens. Matter*, vol. 81, no. 22, Jun. 2010, Art. no. 224410.

[35] W. Yoo, S. Choo, K. Lee, S. Jo, C.-Y. You, J.-I. Hong, and M.-H. Jung, "Exchange bias effect determined by anisotropic magnetoresistance in $CoxNi_{1-x}O/Ni_{0.8}Fe_{0.2}$ bilayer system," *IEEE Trans. Magn.*, vol. 51, no. 11, pp. 1–4, Nov. 2015.

[36] A. E. Berkowitz, M. F. Hansen, R. H. Kodama, Y. J. Tang, J. I. Hong, and D. J. Smith, "Establishing exchange bias below T_N with polycrystalline $Ni_{0.52}Co_{0.48}O$/Co bilayers," *Phys. Rev. B, Condens. Matter*, vol. 72, no. 13, Oct. 2005, Art. no. 134428.

[37] D. Mauri, D. Scholl, H. C. Siegmann, and E. Kay, "Magnetism in very thin films of permalloy measured by spin polarized cascade electrons," *Appl. Phys. A Solids Surf.*, vol. 49, no. 5, pp. 439–447, Nov. 1989.

[38] M. D. Rechtin and B. L. Averbach, "Long-range magnetic order in CoO," *Phys. Rev. B, Condens. Matter*, vol. 6, no. 11, pp. 4294–4300, Dec. 1972.

[39] R. Wu, C. Yun, X. Wang, P. Lu, W. Li, Y. Lin, E.-M. Choi, H. Wang, and J. L. MacManus-Driscoll, "All-oxide nanocomposites to yield large, tunable perpendicular exchange bias above room temperature," *ACS Appl. Mater. Interfaces*, vol. 10, no. 49, pp. 42593–42602, Nov. 2018.

[40] M. D. Stiles and R. D. Mcmichael, "Coercivity in exchange-bias bilayers," *Phys. Rev. B, Condens. Matter*, vol. 63, no. 6, Jan. 2001, Art. no. 064405.

[41] R. Wu, C. Yun, S. L. Ding, X. Wen, S. Q. Liu, C. S. Wang, J. Z. Han, H. L. Du, and J. B. Yang, "A separation of antiferromagnetic spin motion modes in the training effect of exchange biased Co/CoO film with in-plane anisotropy," *J. Appl. Phys.*, vol. 120, no. 5, Aug. 2016, Art. no. 053902.

[42] T. McGuire and R. Potter, "Anisotropic magnetoresistance in ferromagnetic 3d alloys," *IEEE Trans. Magn.*, vol. 11, no. 4, pp. 1018–1038, Jul. 1975.

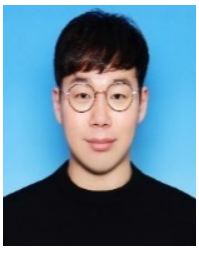

WOOSUK YOO received the B.A. degree in history and the M.S. and Ph.D. degrees from Sogang University, South Korea, in 2012, 2014, and 2020, respectively, both in physics. He is currently a Researcher with Yonsei University, South Korea. His research interests include spintronics, magnetism, and magnetic thin films.

SEONGMIN CHOO received the B.A. and Ph.D. degrees from Sogang University, South Korea, in 2009 and 2015, respectively, both in physics. He is currently a Research and Development Researcher with Samsung Electronics. His research interests include dielectric materials and plasma.

SINYONG JO received the B.A. and M.S. degrees from Inha University, South Korea, in 2012 and 2014, respectively, both in physics. He is currently a Researcher with INNO6. His research interests include spintronics, magnetism, and magnetic thin films.

CHUN-YEOL YOU received the B.A., M.S., and Ph.D. degrees from the Korea Advanced Institute of Science and Technology (KAIST), South Korea, in 1991, 1993, and 1997, respectively, all in physics. He is currently a Professor with the Department of Emerging Materials Science, Daegu Gyeongbuk Institute of Science and Technology (DGIST), South Korea. His research interests include spintronics, nano spin devices, magnetism, and magnetic thin films.

JUNG-IL HONG received the B.A. degree in physics from the Korea Advanced Institute of Science and Technology (KAIST), South Korea, in 1992, and the Ph.D. degree in materials science from Northwestern University, IL, USA, in 1999. He is currently a Professor with the Department of Emerging Materials Science, Daegu Gyeongbuk Institute of Science and Technology (DGIST), South Korea. His research interests include low dimension nano materials, spintronics, nano spin devices, and thin films.

KYUJOON LEE received the B.A. and Ph.D. degrees from Sogang University, South Korea, in 2009 and 2015, respectively, both in physics. He is currently a Postdoctoral Researcher with Johannes Gutenberg University Mainz, Germany. His research interests include spintronics, magnetism, spin-orbitronics, dirac materials, and magnetic thin films.

MYUNG-HWA JUNG received the B.A. and M.S. degrees from Sungkyunkwan University, South Korea, in 1995 and 1997, respectively, and the Ph.D. degree from Hiroshima University, Japan, in 2000, all in physics. She is currently a Professor of physics with Sogang University, South Korea. Her research interests include spintronics, magnetism, dirac materials, and magnetic thin films.